DTU Library

Flange Curling in Cold Formed Profiles

Jönsson, Jeppe; Ramonas, Gediminas

Published in:
Proceedings of Nordic Steel Construction Conference 2012

Publication date:
2012

Link back to DTU Orbit

FLANGE CURLING IN COLD FORMED PROFILES

Jeppe Jönsson, Gediminas Ramonas
DTU Civil Engineering, Technical University of Denmark

Abstract: The non-linear flange curling phenomenon in cold formed profiles is the tendency of slender flanges to deform towards the neutral axis for increasing flexural curvature. Based on Braziers work, Winter proposed a simple engineering formula for determination of the local flange deformation towards the neutral axis. This formula is used in Eurocode to estimate flange curling deformation and give a limit after which flange curling has to be taken into account, however no method or procedure is given for this. The current work presents a new original method, which fits directly into the iterative scheme of Eurocode for determination of effective widths and the neutral axis position in flexure of thin-walled cross sections.

1 Introduction

Recently a general analytical model based on a Brazier type analysis [1] has been presented by Silvestre [2,3], however it does not fit into the iterative scheme for the determination of the flexural properties of thin-walled cross sections with effective widths in compressed flanges.
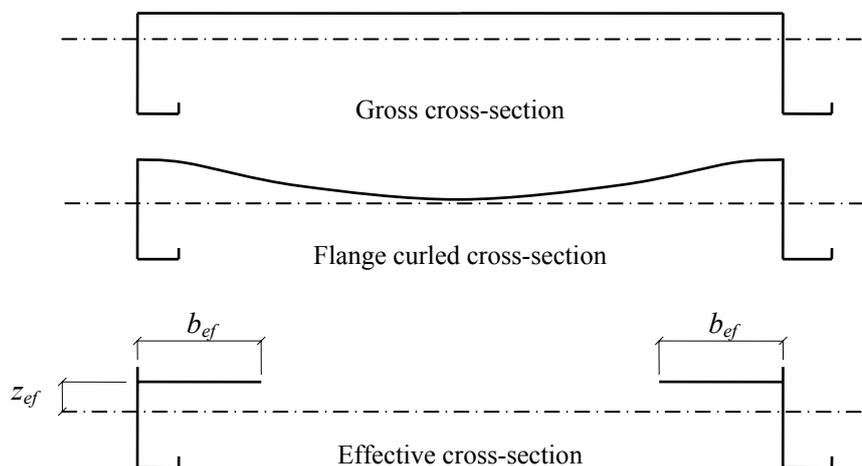

Fig. 1: Flange curling of slender tension flanges

The current work presents a new original flange curling model (FCM), which fits into the iterative scheme for determination of the neutral axis position and section properties of thin-walled profiles with effective widths. The transverse action on the flange is established through knowledge of the current curvature of the beam, the magnitude of flange curling deformation, the current iterated position of the neutral axis and the axial stress distribution in the deformed state. The axial stress distribution in the deformed and flange curled state is based on the primary assumption that also flange curled distorted cross sections remain plane.

This assumption leads to a simple determination of the non-linear deformation in the flange. The presented formulation is based on the principles of Winters formula for flange curling and the integration of the approximated stress distribution in the flange. We introduce effective widths in the tension flange as well as an effective distance from the neutral axis as shown in Fig. 1. The introduction of an effective distance from the neutral axis is a novel idea, which is a natural result of the demand for equivalence of stress distributions. The formulation is developed for tension flanges and since in the case of for slender flanges in compression the buckling deformations govern the behavior and the stress distribution in such a way that conventional Winter's formulas for effective widths can remain unchanged. However in the case of wide compression flanges with stiffeners the flange additional investigations are needed.

Winter [4] was the first to investigate flange curling behavior. His formula is currently adopted by Eurocode 3 – Part 1.3 [5]. Bernard et al. [6] performed experiments with three different slender geometries. The results of these tests will be compared to results found using the finite element program Abaqus and to results obtained with the FCM proposed in this paper. Lecce et al. [7] focus on the support conditions of the flanges and the variation of stresses in the wide flanges caused by the flange curling. Moreover, Lecce was the first to suggest recalculation of moment of inertia due to the transversal deflection of the flange. Silvestre [2,3] created analytical models to study the flange curling phenomenon in the wide flanges. Silvestre also compared his results to the experimental results of Bernard's and Lecce and suggested an analytical model to calculate the effects of nonlinear flange curling. Silvestre also proposed the use of an effective width method. The presented FCM and a number of related models have been developed and investigated by the authors in the master thesis of Ramonas [8].

2 Basic theory of the Flange Curling Model (FCM)

The flange curling phenomenon is initiated by the curvature of the beam, which rotates the axial flange stresses resulting in an internal action component directed towards the neutral axis of the beam as shown in Fig. 2.
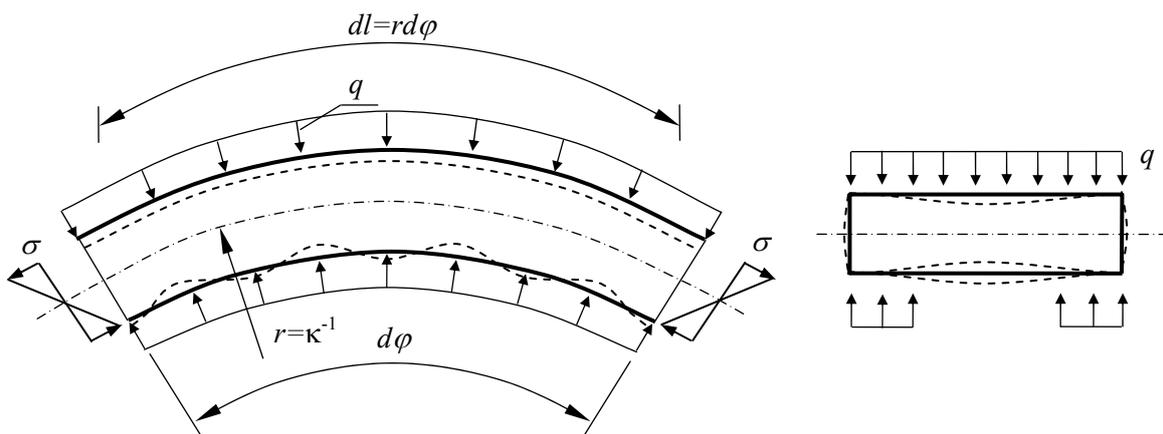

Fig. 2: Second order transverse load action on the flanges

Equilibrium of the axial stresses σ in a curved flange of thickness t in a beam with constant curvature κ gives us that the transverse flange load q is

$$q = t\sigma\kappa \tag{1}$$

This equilibrium based transverse load leads to flange curling deflections of the flange. In the left part of Fig. 2 we have also shown the middle flange displacements as a dashed curve below the upper flange. Assuming that the end cross sections remain plane (no shear lag) we can acknowledge that deflecting the middle part of the flange towards the neutral axis line will lead to shortening of the upper flange corresponding to a reduction of the tension strain. Thus we assume that the strain and stress distribution over the flange curled cross section remains plane and that we can calculate the flange stress using the curling deflection of the flange.

The most practical iteration scheme adopted to find the effective cross section is to iterate the position of the neutral axis, based on the current effective buckling widths and on the effective flange curling widths. The iterated distance from the neutral axis to the edge of the flange considered will be denoted by z_e and the curvature in the current iteration can be found from

$$\kappa = \frac{\sigma_e}{Ez_e} \quad \text{or} \quad \kappa = \frac{M}{EI_{ef}} \tag{2}$$

The edge stress and curvature value stays constant within the iteration. To be able to determine the magnitude of the flange curling load we need to examine the relationship between flange curling load, displacements and the flange stresses as shown in Fig. 3a.
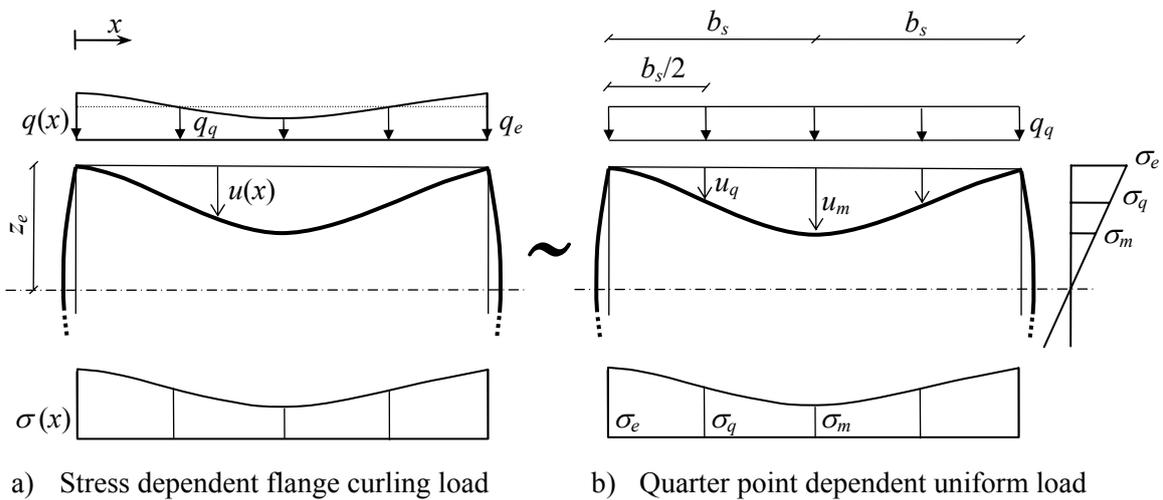

a) Stress dependent flange curling load   b) Quarter point dependent uniform load

Fig. 3: Modelling of second order transverse load action on the flanges.

The main assumption of this model is that "distorted cross-sections remain plain". This leads to the assumption that the stresses in the flanges are directly proportional to the distance from the neutral axis. As the flange curling begins the deflections toward the neutral axis, the axial stresses in the flanges decrease going from the corner joining the flange and the web towards the middle of the flange. The flange stress can thus be determined as a function of the distance x from the corner as:

$$\sigma(x) = \sigma_e \left(1 - \frac{u(x)}{z_e}\right) \tag{3}$$

In which σ_e is the edge stress and $u(x)$ is the curling displacement determined by the loading.

The displacements of the flange could be solved though solution of a more complicated differential equation in which the loading is displacement dependent. However we will simplify the problem as shown in Fig. 3b by assuming that the flange curling load q_q is uniform and determined by the displacements u_q at the quarter points of the flange $x = \frac{1}{2}b_s$ as follows

$$q_q = q_e \left(1 - \frac{u_q}{z_e}\right) , \qquad \text{where } q_e = t\sigma_e \kappa \tag{4}$$

The displacements from a uniform flange load q_q may be found by assuming that the webs stiffen the flange by using the model shown in Fig. 4. In this model we propose to use $s_w = 0.9 h_w$ as the length of the side spans.
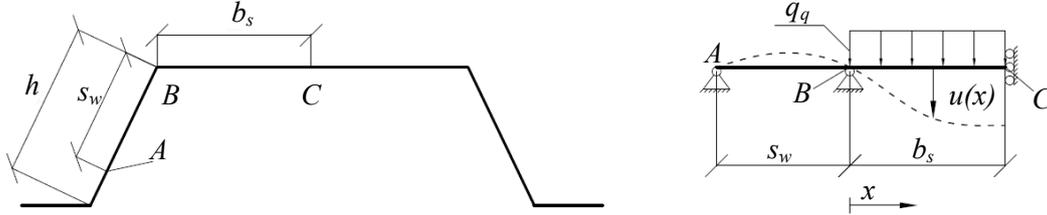

Fig. 4: Curling displacements $u(x)$ based on approximate flange support conditions.

Using ordinary beam statics the flange curling displacements for a uniform load q_q may be found to be

$$u(\xi) = \frac{q_q b_s^4}{3D}\xi\left(1 - \frac{1}{2}\xi^2 + \frac{1}{8}\xi^3 - \frac{(1-\xi/2)}{1+s_w/(3b_s)}\right) , \quad \text{where } \xi = x/b_s \quad \text{and} \quad D = \frac{Et^3}{12(1-v^2)} \tag{5}$$

The deflection at the quarter point $\xi = b_s/2$ can now be found as a function of the uniform load as

$$u_q = C_q q_q , \quad \text{where} \quad C_q = \frac{b_s^4}{24D}\left(\frac{57}{16} - \frac{3}{1+s_w/(3b_s)}\right) \tag{6}$$

Where C_q is the flexibility constant for the flange quarter point. Now we are able to extract the main non-linear flange curling effect by inserting Eq. (4) into Eq. (6) and isolate the displacements as

$$u_q = \frac{C_q q_e}{1 - C_q q_e / z_e} \tag{7}$$

Finally we are able to find the approximated uniform flange curling load by insert this into Eq. (4) as follows

$$q_q = q_e \left(1 - \frac{C_q q_e}{z_e + C_q q_e}\right) \tag{8}$$

With this equation and the use of the fact that the edge load is given by $q_e = t\sigma_e\kappa$ we can find flange curling displacements using Eq. (6) and the flange stress distribution using Eq. (3).

3 Effective widths and effective moment arm of FCM

The effective widths b_{ef} and the effective moment arm z_{ef} can be found by demanding equal moment and normal force for the flange curled cross section with the approximate stress distribution given by the FCM and the stress distribution given by the effective cross section as shown in Fig. 1. To be brief the result of the equivalence consideration is that the effective moment arm z_{ef} and the effective width b_{ef} are given by

$$\frac{z_{ef}}{z_e} = \frac{\int_0^1 \left(1 + \frac{u(\xi)}{z_e}\right)^2 d\xi}{\int_0^1 \left(1 + \frac{u(\xi)}{z_e}\right) d\xi} = \frac{1 - 2\beta_1 + \beta_2}{1 - \beta_1}, \qquad \frac{b_{ef}}{b_s} = \frac{z_{ef}}{z_e} \int_0^1 \left(1 + \frac{u(\xi)}{z_e}\right) d\xi = \frac{z_{ef}}{z_e}(1 - \beta_1) \quad (9)$$

Where the following parameters are have been introduce to ease the calculation:

$$\beta_1 = \frac{1 + 2s_w/b_s}{15\left(1 + s_w/(3b_s)\right)} \left(\frac{q_q b_s^4}{3D}\right) \quad (10)$$

$$\beta_2 = \frac{1}{20160}\left(3968 - \frac{6519}{1 + s_w/(3b_s)} + \frac{2688}{\left(1 + s_w/(3b_s)\right)^2}\right)\left(\frac{q_q b_s^4}{3D}\right)^2 \quad (11)$$

These equations can be directly introduced into the iterative scheme for determination of effective cross-section properties. In the iterative procedure the neutral axis position is known in each iterative step. The current curvature can be determined from Eq. (2) and the quarter point loading from Eq. (8) in which the edge load is determined as $q_e = t\sigma_e\kappa$.

4 Flange curling analysis of three box-shape profiles

To investigate the influence of the wide flange slenderness three different box-shaped profiles have been analysed. The main geometric measures of the box shaped profiles are shown in mm in Fig. 5. The widths b of the box shaped profiles has been chosen as 200mm, 400mm and 600mm. The thickness of the compression flange has been chosen so that it does not exhibit buckling or flange curling during the analysis.
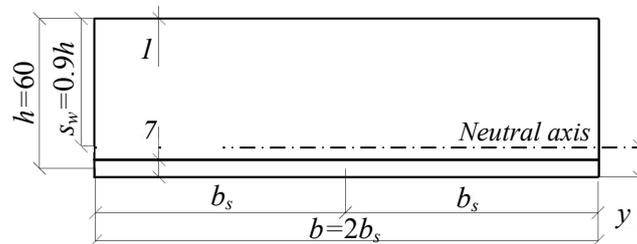

Fig. 5: Box-shape profile with thick lower flange and width $b=2b_s$.

Based on the experiments of Bernard et al. [6] our Abaqus models where originally 4m long with symmetrically place supports 1m from the ends. The end sections where load by transverse forces at the webs and the supports where placed as a line support below the thick compression flange. Thus the central 2m of the profile exhibited constant moment. However as we found that the length of the central span has an influence on the magnitude of the flange curling, thus the central constant moment span length L was varied dependent on the width b of the analysed profile so that the L/b ratio is equal to 10 or 20, while the 1m length of the end cantilevered parts where kept constant. A structured rectangular mesh using S4R elements was chosen with element lengths in the range of 1cm to 2.5cm. The material model used in the Abaqus model is linear with elasticity modulus of $E = 2.1 \cdot 10^5$ MPa and Poisson ratio of $\nu = 0.3$. The analysis performed includes geometric nonlinear deformation contributions, however imperfections have not been included, since they have practically no influence on the curling of the tension flange.

The calculated normalized flange curling displacement u_m/h based on the effective widths and effective moment arm of the FCM are compared to the results of the described Abaqus model as a function of the normalized flange edge stress σ_e/f_y in Fig. 6. The yield stress used for the normalization is $f_y = 350\text{MPa}$. The curves are naturally grouped according to the b/t ratios of 600, 400 and 200. It is seen that the FCM model behaves correctly and that the ideal constant moment situation with flange curling is difficult to model. In Fig. 7 the moment normalized by the gross cross-section moment capacity $M/(W_{\text{gross}}f_y)$ has been plotted as a function of the normalized edge stress σ_e/f_y. This figure also shows the adequate behaviour of the FCM for slender and wide tension flanges. The normalized stress at the midpoint of the flange σ_m/f_y as a function of the stress level is shown in Fig. 8 and it can be seen that the FCM catches the overall behaviour quite well in the practical range of profiles. However as the mid flange stress level increases and passes its maximum value it is seen that the results from the Abaqus models depend on the *L/b* ratio and therefore shows a large spread of the stress results.
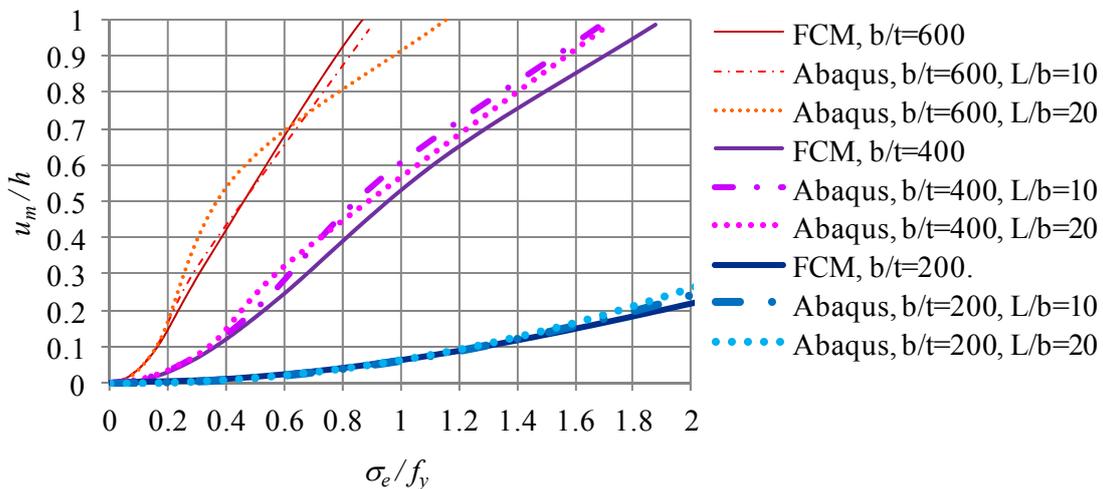

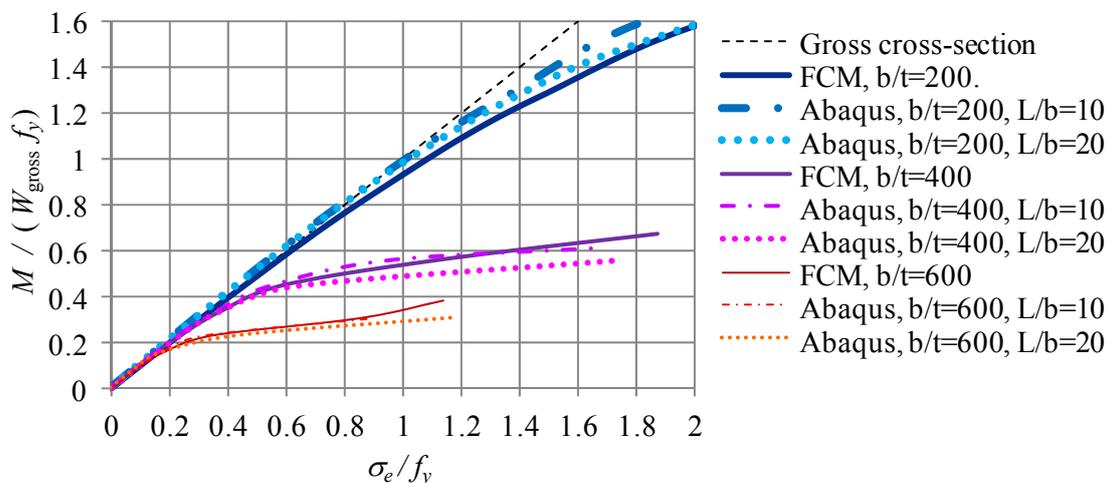**Fig. 6:** FC-displacements as a function of the edge stress for box profiles with various *b/t* ratios.

Fig. 7: Moment as a function of the edge stress for box profiles with various *b/t* ratios.
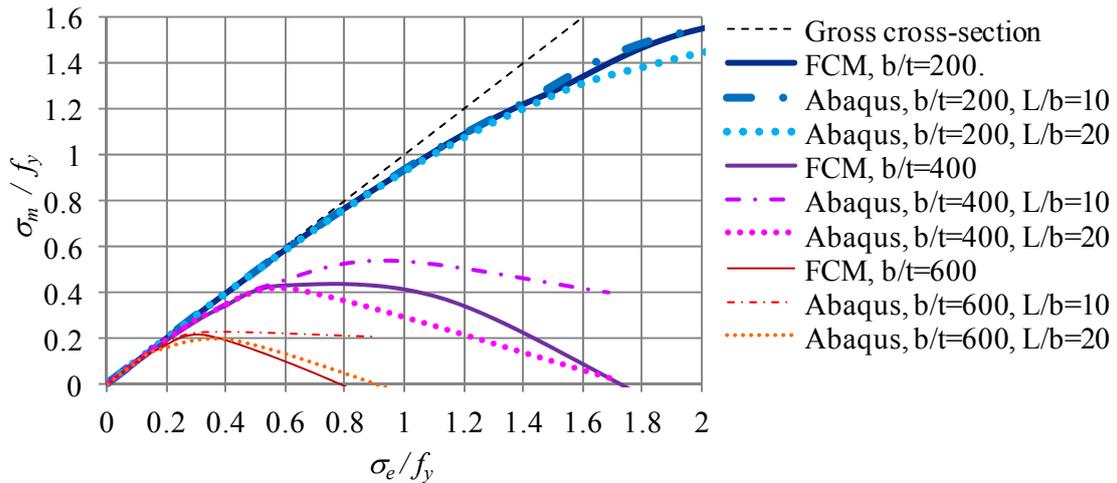
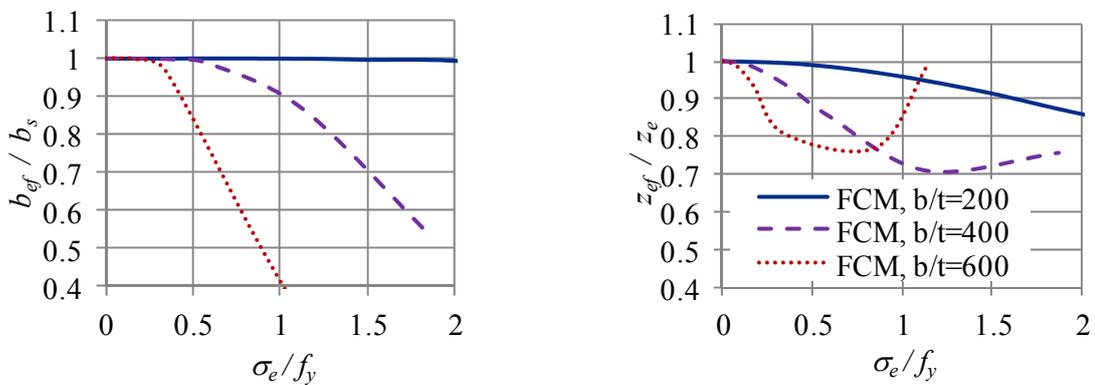**Fig. 8:** Mid flange stress as a function of the edge stress for box profiles with various b/t ratios.

Fig. 9: Effective width and its position as a function of σ_e for box profiles with various b/t ratios.
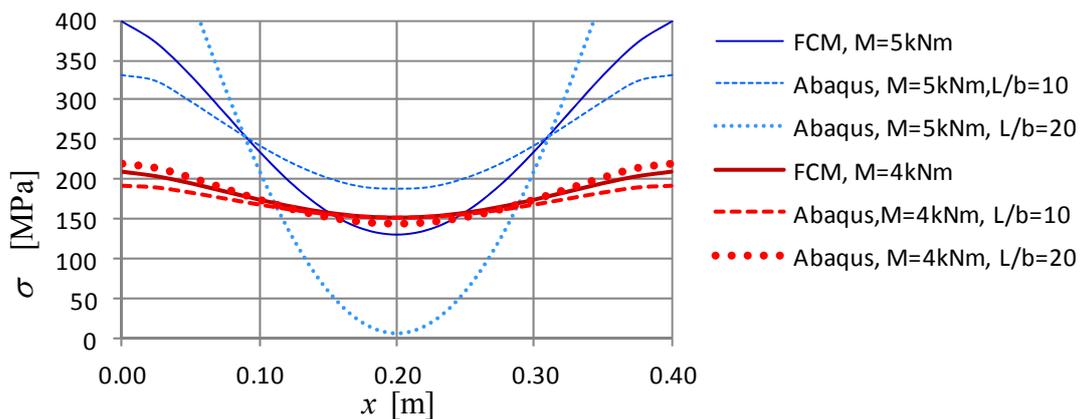

Fig. 10: Stress distribution in the flange for b/t=400 using FCM and Abaqus.

Plots of the relative effective width and the relative effective moment arm as a function of the relative stress level are shown in Fig. 9. It is seen that as the stress level increases the moment arm is reduced followed a little later by the reduction of effective width, however as the width reduction becomes larger, then the effective moment arm may increase again. In Fig. 10 a plot of the stress distributions for two stress levels are shown for the FCM model and compared to the stresses of the Abaqus model for the box-shaped profile with b/t=400. It is seen that the

stress distribution found in the Abaqus model depends on the L/b ratio and that deviating results are found at high stress levels and large flange curling deflections.

5 Analysis of a liner tray with a wide tension flange

Bernard [6] used the cold-formed standing seam panels consisting of two upstands with simple folded lips and wide central flanges. These profiles are called Condeck and are used as liner trays or so-called Cassettes. The geometry and general dimensions of the specimen considered in this paper is illustrated in Fig 11a.

A simplified profile geometry is used for the calculations and analysis in this work. Fig. 11 shows the simplified geometry to the right. Bernard [6] made two types of the experiments. He examined the behavior of wide flanges in tension and compression under the pure bending conditions of the profile. Due to the fact that intermediate stiffeners are omitted in the simplified geometry, the results only from the tension tests will be used. Bernard [6] examined different number of Condeck profiles connected together side by side. The webs of the flanges of the central panels were not able to sway sideways because the webs of the adjacent profiles acted in opposite directions and restrained each other. Based on this condition a model has been created in Abaqus in which the bottom outstand flanges are restrained agains transverse displacements. Fig. 12 represents the deflections of the middle of tension flanges, which were caused by the flange curling. The results from Bernard's experiment are the thin lines. They comply with the results of the finite elements analysis.
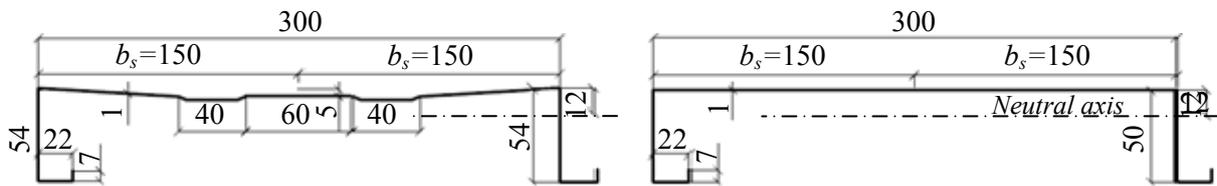

Fig. 11: a) Original and b) simplified geometry of the Condeck profile used in the present work.
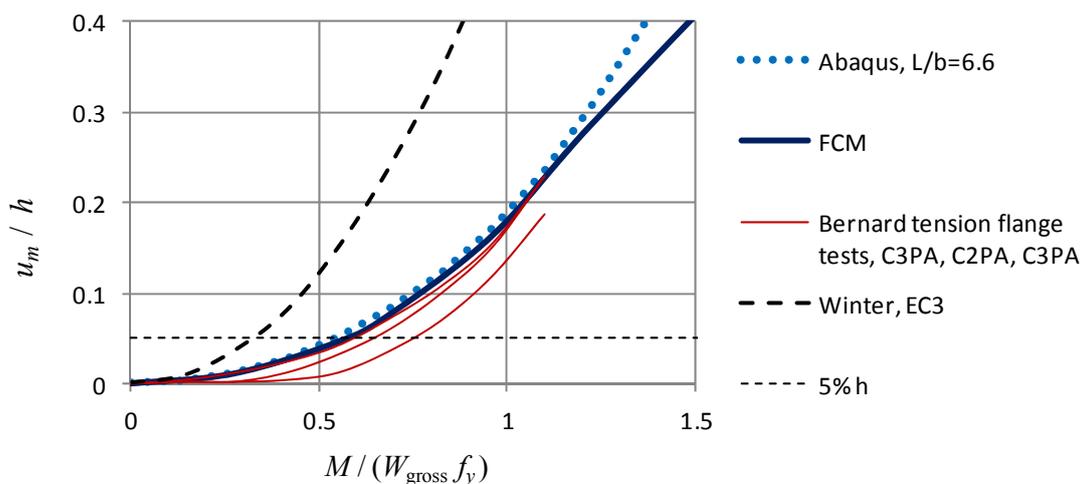

Fig. 12: FC displacements of Condeck profile compared to Bernard tests and Abaqus.

6 Analysis of trapezoidal sheeting in positive bending

In the paper by Bernard et al. [6] he also presents results from experiments with a trapezoidal sheeting. Pure bending was applied to the sheeting with the upper flange in compression and the lower flange in tension. The geometry of one module width of the sheeting is depicted in Fig. 13. The upper flange has an intermediate stiffener and the full developed width of this flange ("unfolded flange") is used in the FCM calculations. Bernard used a single sheeting panel consisting of three troughs (modules) in his experiments. He made two tests and measured the deflections of every flange. However, he did not fixed the outer edges of the specimens against the sideways "sway" expansion. For this reason the specimen behavior in his tests is not equivalent to that of conventional sheeting with edge seems. The Abaqus model which has been used in the present work is however restrained against lateral movement of the outer flanges. Since our non-linear Abaqus analysis was performed without imperfections the analysis stopped at a load level corresponding to initiation of local buckling in the flat widths of the upper flange. In the experiments, FCM and Abaqus analyses the lower flange experienced some flange curling deflections. These deformations are relatively small, because the flange width has a large influence on the magnitude of the deflections, which are lower than 5% of the profile height. Due to this fact the displacement measurements which were found by Bernard may be not very precise. In Fig.14 we have shown the deflections found using the FCM model and compared these to the experimental test results of Bernard. Furthermore, since Silvestre [3] has also investigated this trapezoidal sheeting profile, we have included his results in the plots shown in the figures.
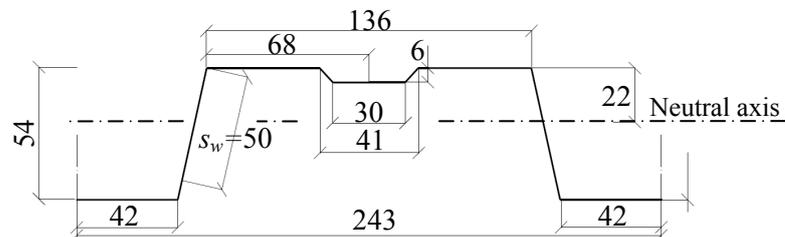

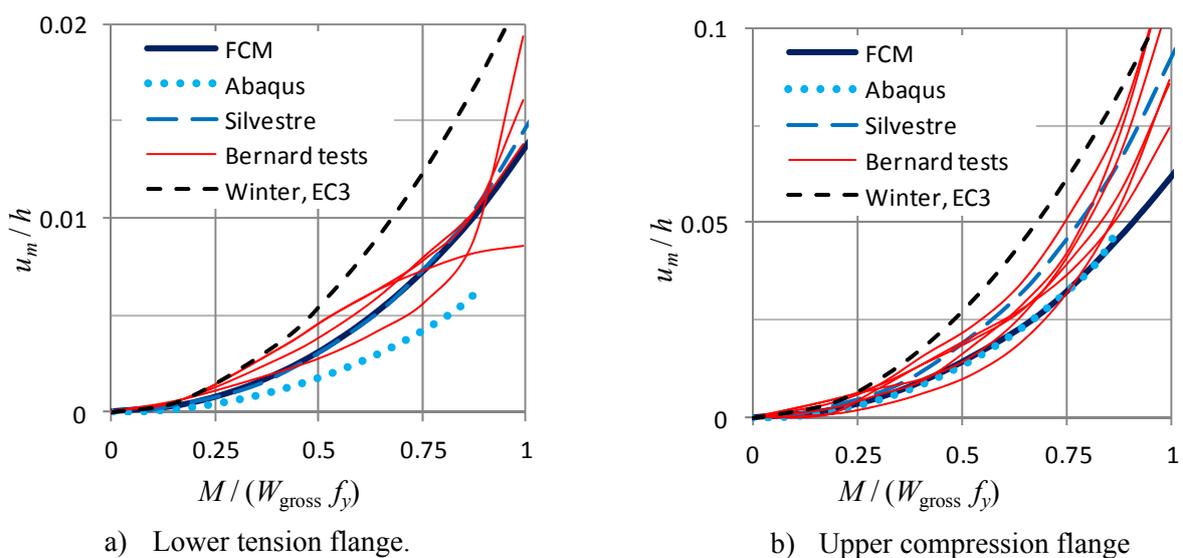**Fig. 13:** Geometry of trapezoidal profile test by Bernard.

a) Lower tension flange.   b) Upper compression flange

Fig. 14: FC displacement in the flanges of the trapezoidal profile

6 Conclusions

The proposed flange curling method FCM, which fits directly into the iterative scheme of Eurocode [5] for analysis of effective cross-sections, seems to be very promising and it has been shown that:

1. The FCM reproduces the non-linear flange curling displacement behaviour for tension flanges for a practical range of slenderness values;
2. The FCM approximates the stress distribution in the curled flange with reasonable accuracy.
3. Effective moment arm reduction and effective widths have been given for wide tension flanges
4. Stiffeners in tension flanges are taken into account by using the full developed width of the flange.
5. Further research into the use of the FCM for compression flanges is needed.

However with respect to the last point preliminary investigations show that for compression flanges without stiffeners flange curling is not an issue and for flanges with stiffeners flange curling can be analysed by using the reduced stress level in the (buckled) stiffener, $\chi\sigma_{com}$, to determine and replace the "quarter" point load, i.e. $q_q = t\chi\sigma_{com}\kappa$ and introduce an effective moment arm $z_{s,ef}$ for the stiffener. It is believed that this FCM method with the derived effective width will help assessing the carrying capacity of slender liner trays and slender wide flanged trapezoidal sheeting.

References

[1]   Brazier L. G. "On the flexure of thin cylindrical shells and other "thin" sections", *Proceedings of the Royal society of London. Series A, containing papers of a mathematical and physical character*, Vol. 116, No. 773, 104-114, 1927.

[2]   Silvestre N. "Non-linear curling of wide single-flange steel panels", *Journal of construction steel research*, No. 65, 509-522, 2009.

[3]   Silvestre N. "Analytical model to study the curling phenomena in wide flange trapezoidal panels", *Engineering structures*, No. 29, 3443-3454, 2007.

[4]   Winter G. "Stress distributions in and equivalent width of flanges of wide, thin-wall steel beams", *Technical notes, National advisory committee for aeronautics*, No. 784, 1-27, 1940.

[5]   EN 1993-1-3. *Eurocode 3: Design of steel structures. Part 1–3: General Rules. Supplementary rules for cold-formed thin gauge members and sheeting.* Published by European Committee for Standardization, Brussels, 2006.

[6]   Bernard E. S., Bridge R. Q. "Flange curling in profiled steel decks", *Thin-walled structures*, No. 1, Vol. 25, 1-29, 1996.

[7]   Lecce M., Rasmussen K. JR. "Nonlinear flange curling of wide-flange sections", *The University of Sydney, department of civil engineering. Research report*, No. R850, 1-31, 2005.

[8]   Ramonas G. "Flange curling in thin-gauge Profiles". *Master Thesis, DTU Civil engineering, Technical University of Denmark,* March 2012.